Geoderma Regional 42 (2025) e00989

Contents lists available at ScienceDirect

Geoderma Regional

journal homepage: www.elsevier.com/locate/geodrs

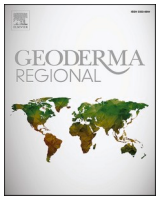

Assessing the morphological, physicochemical, and mineralogical properties of black soils and ferralsols and identification of potential risk of degradations along a climotoposequence in Foumbot, West Cameroon

Georges Martial Ndzana [a,*], Jeroen Meersmans [b], Li Huang [c], Tabi Fritz Oben [a], Etienne Mboua [a], Azinwi Primus [a], C.T. Kaamil Fonfatawouo [a], Danielle Mamba [d], Etienne Bekoa [e], Bertrand Mungu Akam [f], Joseph Kabala Mubolo [a], Bin Zhang [g]

[a] Department of Soil Sciences, Faculty of Agronomy and Agricultural Sciences, University of Dschang, Po. Box 222, Dschang, Cameroon
[b] Department of Gembloux Agro-Bio Tech, University of Liège, Liège 4000, Belgium
[c] Key Laboratory of Arable Land Conservation (Middle and Lower Reaches of Yangtze River), Ministry of Agriculture, Huazhong Agricultural University, Wuhan 430070, China
[d] Doctorate school for pure and Applied Sciences, University of Douala, Cameroon
[e] Department or Earth Sciences, University of Yaoundé I, Yaoundé, Cameroon
[f] China University of Geosciences Wuhan, 388 Lumo Rd, Hongshan, Wuhan, Hubei 430079, China
[g] College of Resources and Environmental Sciences, Nanjing Agricultural University, Nanjing 210095, China

ARTICLE INFO

Keywords:
Climate gradient
Soil morphology
Soil mineralogy
Soil classification
Soil toposequence

ABSTRACT

Foumbot in Cameroon is renowned for its fertile soils, which serves as a food basket for the region. However, these soils are currently under threat due to climate change and overutilization. As such, there is a need to better understand their properties, variability and identify the degradation risks to improve their management and conservation. To address this gap, soil profiles formed under volcanic deposits were sampled at three distinct altitudes: 1156 m (highland), 1075 m (middle land), and 974 m (lowland), representing tropical highland, transitioning tropical highland, and tropical forest climates, respectively. Physical and chemical analyses, X-ray diffraction (XRD) and Fourier-Transform Infrared (FTIR) techniques, were conducted to determine the variability of soil morphology, physical and chemical properties, and mineralogy as well as soil classification under climotoposequence. The findings reveal that pedon 1 in the highland was dark in colors (2.5Y and 10YR), slightly acidic to neutral and exhibited the highest organic carbon content (6.8 %) in the surface horizon. In contrast, the middle land, showed a slightly acidic profile (pedon 2) characterized by a darker surface horizon (10YR) with a yellowish subsoil (7.5YR) and lower organic content (4.1 %) in surface horizon compared to pedon 1. Finally, the lowland profile (pedon 3), displayed more acidic conditions and the lowest soil organic carbon content (2.5 %) in surface horizon compared to pedon 1 and pedon 2. A trend of decreasing Alo + ½Feo and Alp/Alo alongside increasing clay content was observed with decreasing altitude. Mineralogical analysis revealed a transition from short-range ordered minerals (allophane and ferrihydrite) in highland soils to poor crystalline kaolinite dominance in the middle land and well crystalline kaolinite in lowland. Additionally, bulk density increased with decreasing altitude. According to the WRB classification, Pedon 1 was classified as Mollic Vytric Silandic **Andosol** (Loamic, Eutrosilic, Humic), Pedon 2 as Dystric Xanthic Andic **Ferralsol** (Clayic, Humic), and Pedon 3 as Umbric Rhodic **Ferralsol (**Clayic, Humic). Andosol was identified as black soil and presents greater potential for agricultural productivity compared to the two other pedons. Since andosols are situated at the top of the hill, possess structural weaknesses (granular structure), and are subjected to intensive cultivation, they pose a higher potential risk of degradation when farming is practiced compared to the other two pedons. This study highlights the significant influence of pedogenetic factors on the soil properties and mineral composition and reveals the urgent need of adopting new soils sustainable management strategies to protect black soils in the Foumbot region of Cameroon.

* Corresponding author.
E-mail address: ndzanageorges2006@yahoo.fr (G.M. Ndzana).

https://doi.org/10.1016/j.geodrs.2025.e00989
Received 30 December 2024; Received in revised form 26 June 2025; Accepted 21 July 2025
Available online 21 July 2025

1. Introduction

Soil is a fundamental resource for sustaining life on Earth. It acts as a habitat for diverse organisms and provides essential ecosystem services such as nutrient cycling, carbon storage, climate regulation and global food security (Daily et al., 1997; Ehrlich et al., 1993).

Pedogenesis leads to the development of soils with a wide variation in properties along soil sequences (Candra et al., 2023; Rezaei et al., 2015). The distribution of soil properties often depends on the natural factors involved in soil formation. Increasing numbers of studies were conducted to determine the key natural factors driving the diversity of soil properties on the various landscape (Miller et al., 1988; Tematio et al., 2009). Among them, topography had been pointed as one of the key natural factors controlling soil formation processes. Elevation, slope, and aspect are the main topography elements that can contribute to the development of soils (Huang and Li, 2024; Geoffry Milne, 1935). For instance, the study of Rezaei et al. (2015) revealed significant effect of slope positions on thickness of the soil profile and solum, clay, organic carbon and total nitrogen percentages and cation exchange capacity. Similarly, Hailemariam et al. (2023) found a significant positive correlation between elevation and soil organic carbon (SOC), soil organic matter (SOM), total nitrogen (TN), cation exchange capacity (CEC), and exchangeable Mg^{2+}; they increase as elevation increases. Topography may also indirectly influence the soil's properties. Indeed, topography features affect runoff, drainage and soil erosion, which in turn drive the soil property variation and consequently control soil formation under a hill slope (Anwar, 2014; Dessalegn et al., 2014).

Climate gradients have also an influence on soil formation processes. Different climate gradients can lead to various soil properties. For instance, the studies of Candra et al. (2023) on the volcanic slopes identified a varied soil types with different mineralogy in the pronounced altitudinal zonation from arid lowlands to humid highlands across the slopes, highlighting the climate variation as one of the primary drivers of mineralogical and pedogenic changes. Weathering of parent materials, which are central to the formation of soil profiles and nutrient availability, are highly influenced by various climatic factors (air temperature, water balance, and annual precipitation) which dictate their intensity and direction, as well as chemical and biological reactions that occur in soils (Lesovaya et al., 2012; Rubinić et al., 2015). Similarly, the study of Tsai et al. (2010) demonstrated the strong influence of climate on pedogenesis in subtropical volcanic landscapes.

Time is also a critical factor affecting pedogenesis in nature. Soil morphological and physicochemical properties were reported to be influenced by age (Stevens and Walker, 1970). For instance, Nayak et al. (1999) reported that among the different morphological properties, the soil color clearly brought out the differences in soil development with age. Numerous natural soil chronosequence have been analyzed to demonstrate the changes in soil properties over time as well as the rates and patterns of soil formation processes (e.g., Bernasconi et al., 2011; Crews et al., 1995; He et al., 2008).

Vegetation plays an active and critical role in the formation of soils. The type of vegetation present has a notable influence on parameters such as the physical properties of surface soil, the chemical properties such as pH parameter, and the degree of leaching or accumulation of base cations (Hailemariam et al., 2023; Hartemink and Barrow, 2023), the quantity and nature of soil organic matter (Bojko and Kabala, 2016; Ghani et al., 2023; Joshi and Garkoti, 2023), and biological activity (Gutiérrez-Girón et al., 2015; Molina et al., 2024; Wang et al., 2024).

Foumbot is part of the Noun Plain belonging to the Volcanic Line of Cameroon. This plane rises to an average altitude of 1100 m above sea level. As elevation increases, soil development tends to be slower because of the variation of climate and thinner vegetation cover. In Foumbot, soils are considered fertile mainly because they have been formed from the weathering and decomposition of volcanic rocks, which provide minerals and nutrients that support plant growth (Tchokona Seuwi, 2010; Wandji et al., 2000). Some of these soils present a very thick and dark surface horizons ($\geq$ 25 cm) with a soil organic content $\geq$0.6 %, which fit the definition of tropical black soils as developed by the INBS/ITPS-FAO (FAO, 2019). In the global landscape of food security and climate crisis, black soils emerge as a key solution for mitigating climate change and enhancing agricultural productivity. These soils are critically important due to their high soil organic carbon (SOC) sequestration potential, storing 8.2 % of the world's SOC stock (Krasilnikov et al., 2022). Despite their strategic importance, black soils in Sub-Saharan Africa remain severely under-studied. The latest United Nations report on the worldwide condition of black soils highlights the lack of data and understanding of black soils properties and management strategies in Africa (Krasilnikov et al., 2022). This scientific gap limits our understanding of degradation processes and restricts awareness among farmers, extension agents, and policymakers. It also undermines efforts to design targeted and evidence-based conservation policies (Montanarella et al., 2021). Many studies were reported on soils from Foumbot. Some studies were focused on the soil erodibility in the area (Fokeng et al., 2020; Ngandeu-Mboyo et al., 2016; Olivier et al., 2023), others in agronomic suitability and fertility aspects (Kunghe et al., 2023; Olivier et al., 2023; Tchekambou et al., 2014) or mineralogy and geochemistry of clay deposits (Mefire et al., 2018). However, the variation of soils properties across the landscape of Foumbot remains unclear, given that the soils properties across the slope exhibit a notable degree of variability as the soil-forming factors can vary considerably over short distances (Sisay et al., 2024) Moreover, research on the properties of black soils in this region are still underdeveloped.

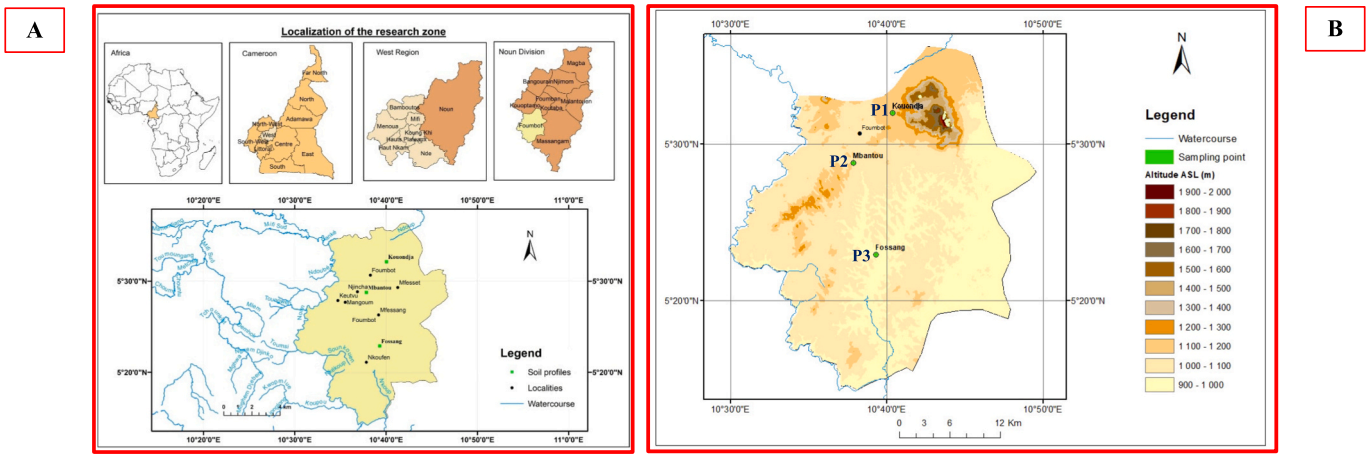

Fig. 1. Localization (A) and geomorphology (B) of the study area; P1= Pedon 1; P2 = Pedon 2; P3= Pedon 3

Table 1
Basic characteristics of the study area.

Soil types	Depth (cm)	Localization	Elevation (m asl)	Vegetation	Climate	Land use
Pedon 1	150	N05°32′07.7″ E010°40′03.8″	1156	Banana, cassava, fern plants, trees.	Tropical Highland	Polyculture, crop rotation,
Pedon 2	150	N05°28′45.9″ E010°37′51.4″	1075	Maize, cassava, okra, banana plants, oil palm, trees.	Transitioning Tropical Highland	Slash/burn, crop rotation, polyculture
Pedon 3	150	N 05°22′53.3″ E010°39′18.8″	974	Tomato, maize, and cassava plants, oil palm, and trees.	Tropical Rainforest	Fallow, slash/burn, crop rotation, polyculture, agroforestry

Therefore, the aim of this study is to analyze the distribution of the soil properties (morphology, physical, chemical and mineralogical properties) of black soils and other soil types and classify soil Pedon along the climotoposequence in Foumbot. Moreover, the study will identify the higher potential risk of soil degradation in the study area. The understanding of the distribution of soil properties across elevations is crucial for identifying areas with higher potential of soil degradations, designing appropriate land use, and managing soil resources sustainably (Marta et al., 2023; Rogora et al., 2018).

2. Material and methods

2.1. Environmental features

The Foumbot region is part of the Noun Plain, belonging to the Cameroon Volcanic Line (CVL) and covers an area of 800 km^2 (Bidias et al., 2023; Ziem à Bidias et al., 2020). Geographically, Foumbot is in the western part of Cameroon, Central Africa, approximately 150 km northwest of the capital city, Yaoundé (Fig.1b). The region is characterized by a diverse climate influenced by its altitude, topography, and proximity to various geographical features. Therefore, as altitude increases, there is a noticeable decrease in temperature and variations in precipitation patterns. The Pedon1 profile (P1) was formed at 1156 m of altitude, the Pedon 2 (P2) at 1075 m of altitude, and the Pedon 3 (P3) at 974 m above sea level (Fig. 1).

According to the Köppen climate classification system, in the altitude bellow 975 m (lowland), the climate is classified as tropical rainforest, typically warmer, with average temperatures of 27 °C, receiving significant rainfall, particularly during the rainy season (April to October), averaging at 2000 mm annually.

At the altitude of 1075 m (middle land), the climate is transitioning towards tropical highlands due to the elevation effect which results in cooler temperatures than at 975 m altitude, with average temperatures of 20 °C and precipitation like that of 975 m altitude with total annual rainfall still high.

At the 1156 m altitude (highland), the climate is strongly classified as tropical highland with average temperature of 15 °C which varied greatly throughout the year, with a clearer dry season, and the average annual rainfall of 2500 mm.

The primary vegetation in the study area before transforming into agricultural land was savanna vegetation in lowland including grasses and sporadic tree species adapted to the drier components of the climate; grasslands in middle land are dominated by various grass species, particularly when the area experiences lower moisture levels, and forests vegetation in highland. The geology of the area revealed the Mbépit Massif, recognized as one of the oldest volcanoes along the Cameroon Volcanic Line, emerged during the Eocene epoch, with 40 K/40Ar dating indicating ages of approximately 45.5 and 44.0 million years. This massif primarily consists of rhyolitic domes and substantial flows of thick, viscous lava (Wandji et al., 2000, 2008).

2.2. Study sites and soil sampling

Three sampling sites were selected in the Foumbot region, spanning across different climatic gradient and elevation from the Northern to Southern areas. These sites, namely Kouondja (N05°32′07.7″E010°40′03.8″), Mbantou (N05°28′45.9″E010°37′51.4″), and Fossang (N05°22′53.3″E010°39′18.8″), represent tropical highland, transitioning tropical highland, and tropical rainforest climate zones, respectively.

Vegetation on the selected sites is reported in Table 1. Soil profiles with three replicates were excavated at each of the three study sites ($n = 3$). The parent material of soil in study areas consists of volcanic deposits, given their locations near the Mbépit Massif and other volcanic formations of the Cameroon Volcanic Line.

The representative soil profiles from Kouondja, Mbantou, and Fossang were named as Pedon1 (P1), Pedon 2 (P2), and Pedon 3 (P3), respectively. Each soil profile was excavated to a depth of 1.5 m and different soil horizons have been identified and carefully described in detail according to the WRB soil classification system (IUSS Working Group WRB, 2022) to obtain the morphological properties and soil types. Samples of the different soil's profiles were collected and air-dried before being gently crushed using a wooden rolling pin and passed through a 2-mm sieve to remove coarse fractions prior to further analysis.

2.3. Laboratory analyses

Soil pH was measured using the 1:2.5 soil-to-water ratio method. Soil organic carbon (SOC) was determined using the wet oxidation method (Walkley and Black, 1934) and the soil organic matter (SOM) was calculated by multiplying the organic carbon content by the van Bemmelen conversion factor of 1.724. This approach to determine SOC was successively used previously in the literature (Liu et al., 2024; Salazar et al., 2024). The total Nitrogen was determined by the digestion with H_2SO_4 using the Kjeldahl method(Jones Jr, 1991). Available phosphorus (P) was determined by Bray II methods (Sims, 2000). The ammonium acetate (1 M and pH 7.0) method was used to determine cation-exchange capacity (CEC) (Metson, 1957). Particle size distribution was determined by Robinson pipette method (Klute, 1986). The bulk density was determined following the Blake Undisturbed Core Method (Blake, 1965). The carbon stocks were calculated in this study according to the method described by Batjes (1996). The values of SOC for each soil type were multiplied by the bulk density and the standard depths.

$$C - stock = C \times BD \times Depth$$

C-stock is measured in kg.ha $^{-1}$; C is measured in %; BD is measured in g/cm^3; Depth is measured in cm. This approach was successfully used in previous works (i.e. Dincă et al., 2015; Huang et al., 2024).

Selective extractions were performed to isolate the Al and Fe-bearing phases present in the soil samples. The citrate bicarbonate-dithionite mixture (CBD) method was used for the extraction of total free iron

Table 2
Profile descriptions of studied soils.

Soil types	Layers	Depth (cm)	Color	Structure	Texture	Porosity	Rooting pattern
	A	0–30	2.5Y,3/1	Fine granular	Loam	High	
	Bw	30–70	2.5Y,3/2	Sub-granular	Sandy Loam	Moderate	
	C	70–100	10YR,4/2	Granular	Sandy Loam	Moderate	Deep
Pedon 1	AC	100–120	10YR,3/1	Granular	Loam	High	
	2Bw	120–150	10YR,3/1	massive	Loam	High	
	A	0–20	10YR,3/2	Fine granular	Clay Loam	Moderate	
	AB	20–80	7.5YR,5/6	Angular Blocky	Clay Loam	Moderate	
Pedon 2	B1	80–100	7.5YR,4/6	Angular Blocky	Clay	Low	Shallow and dense
	B2	100–150	2.5YR,5/8	massive	clay	Low	
	A	0–10	2.5YR,4/4	Thin granular	Clay	Low	
Pedon 3	AB	10–30	2.5YR,4/6	Massive	clay	Low	Shallow and dense
	B	30–140	2.5YR,5/8	Massive	Clay	Low	

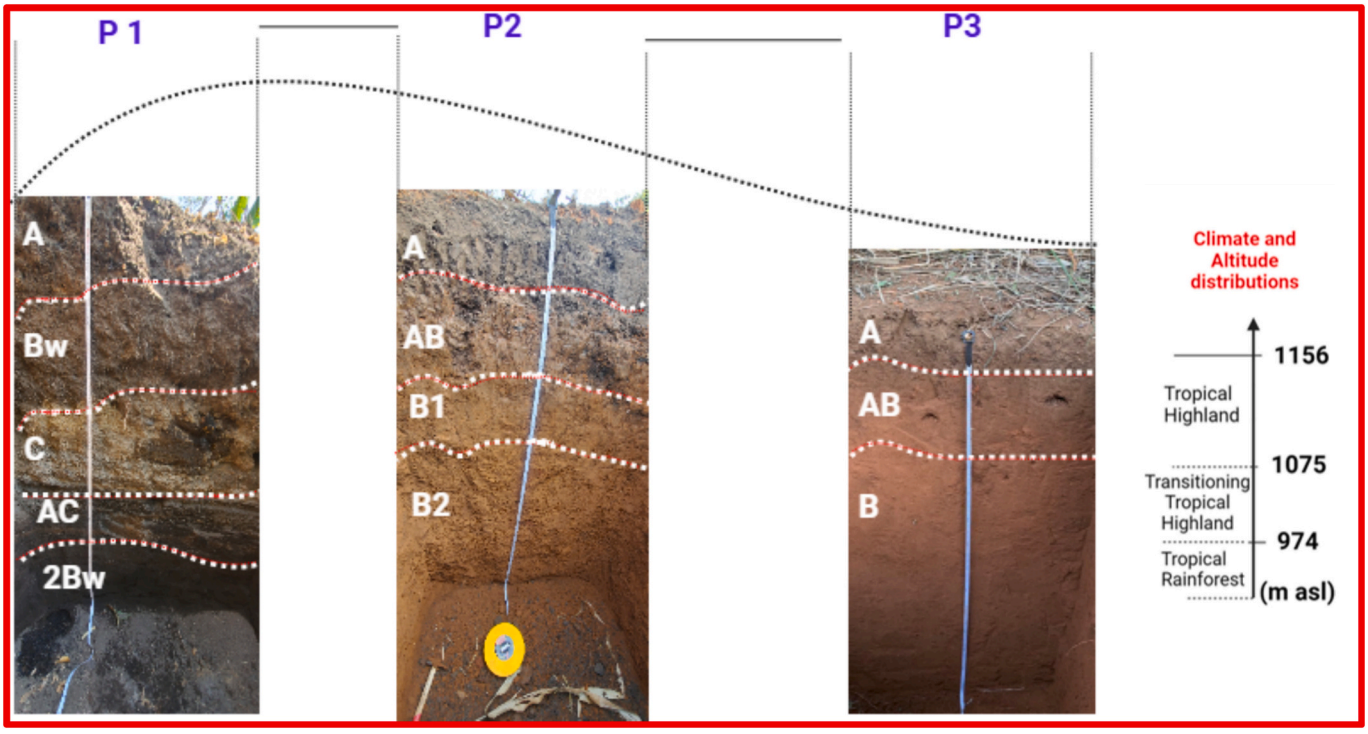

Fig. 2. Morphology of various profiles of pedons along the toposequence. P1=Pedon 1; P2=Pedon 2; P3=Pedon

(Fed) and aluminium (Ald) oxides (Mehra and Jackson, 1960). Meanwhile, the ammonium oxalate solution was employed for the oxalate extractable forms of Fe (Feo) and Al (Alo) oxides (McKeague and Day, 1966). Finally, the sodium pyrophosphate solution was used to extract amorphous organic forms of Fe (Fep) and Al (Alp) oxides (McKeague, 1967).

The Alo and Feo extracted through the ammonium oxalate method come from short-range-order (SRO) minerals such as allophane and imogolite, as well as organically bound Al/Fe. Alo and Feo are considered the active fractions of Al and Fe respectively, which is used as a criterion for andic soil properties. Al and Fe extracted through the pyrophosphate method (Alp and Fep) are typically associated with organic matter to form organo-metallic complex. We assume that (Alo − Alp) and (Feo − Fep) are mainly derived from SRO minerals. The free Fe (hydr)oxides, including crystalline and SRO phases, as well as organically bound Fe, are extracted by the dithionite-citrate method (Watanabe et al., 2023). However, due to the limited selectivity of the methods used, there may be some uncertainty in interpreting the extracted Al/Fe fractions (e.g., Alp and Fep may include small particles of Al/Fe (hydr) oxides that are not bound to organic matter)(Van Ranst et al., 2019; Watanabe et al., 2023). The percentage of ferrihydrite is calculated using the formula: Ferrihydrite (%) = 1.7 × Feo (Childs et al., 1986; Enang et al., 2019). Similarly, the percentage of allophane is determined by the equation: Allophane (%) = 7.1 × Si_o (Poulenard and Herbillon, 2000).

The clay minerals composition was determined by the conventional X-ray diffraction (D8 Advance, Bruker, Rheinstetten, Germany) using CuKα radiation (λ = 1.5418 Å) generated at 40 kV and 40 mA. The powder analysis was used to determine the mineral composition in the bulk soils and the oriented analysis to determine the mineralogy in the clay fraction. Prior to XRD analysis of minerals in clay fraction, an aliquot of the clay sample was treated with Mgcl2 and glycerol solvation (Mg-gly) and a second Aliquot was treated with potassium (K) and subjected to XRD analysis after heating at 25, 350 and 550 °C (Jackson, 1973). For the powder samples of bulk soils, the XRD spectra were recorded in a continuous mode from 29 = 3° to 85° with 0.01° steps at a scanning rate of 2° min^{-1}. The identification of clay minerals and the estimations of their semi-quantitative proportions were performed as reported previous studies (Ndzana et al., 2019).The XRD spectra were analyzed using the MDI Jade 6 and Origin 2018 software.

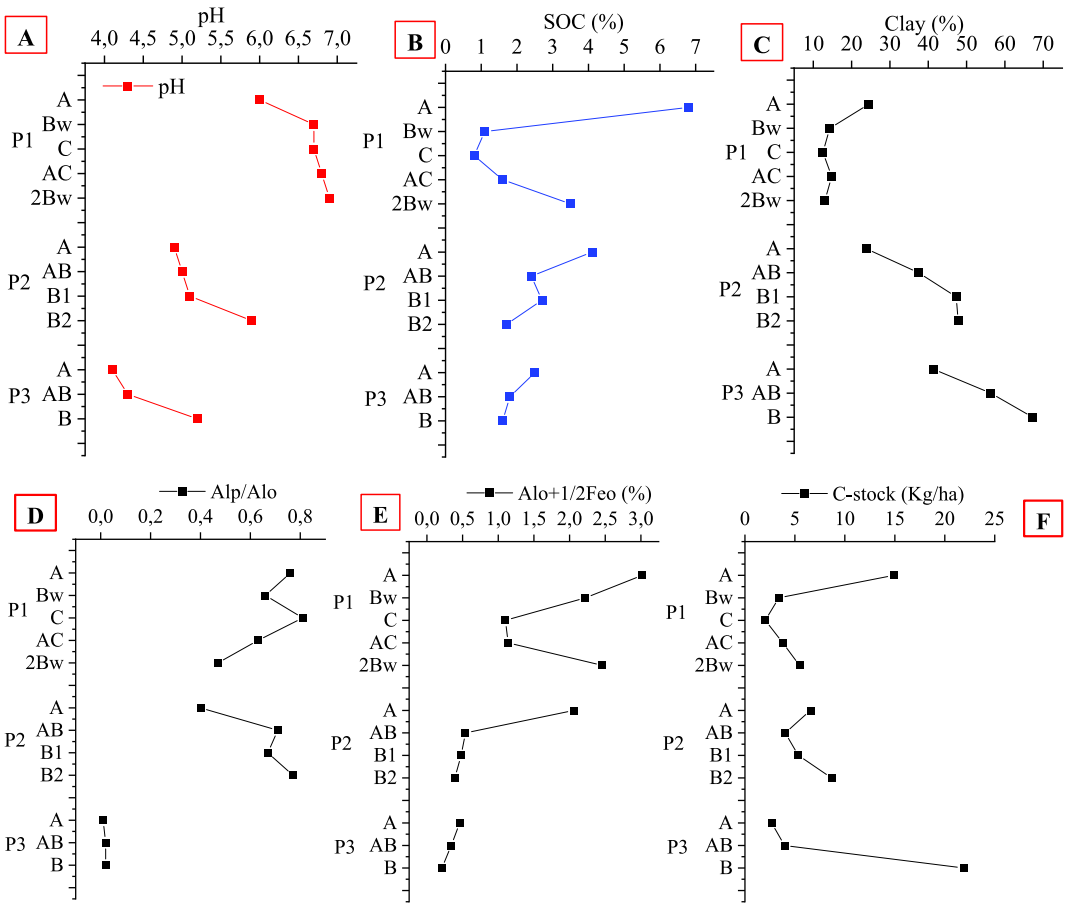

Fig. 3. The distribution of soil physical and chemical properties with depth along the elevation gradient. Error bars indicate standard deviation; Alo and Feo = oxalate-extractable Al and Fe; Alp = pyrophosphate-extractable Al; CEC = cation exchange capacity; OC = Organic carbon. A= pH; B = SOC; C = Clay; D = Alp/Alo; E = Alo + 1/2Feo; F = C-stock

3. Results

3.1. Soil morphology

The color of the P1 profile was predominantly dark gray, apart from the Bw horizon with gray hue, and the C horizon with a light brown hue. Interestingly, this dark color was also observed in the surface horizon (A horizon) of the Pedon 2 profile, whereas the underlying horizons (AB, B1 and B2) had a strong brown color. In contrast, the Pedon 3 had a reddish color throughout its profile (Table 2 and Fig. 2). Pedon 1 exhibited granular structures throughout its depth, except in the 2Bw horizon, while Pedon 2 had a granular surface and blocky subsurface horizons, and Pedon 3 was characterized by a granular surface with massive subsurface horizons. The texture of the Pedon 1 is loamy and varied from sandy to clay loamy as we shifted from Bw and C horizons to AC and 2Bw horizons. Pedon 2 exhibited a clayic texture in most of the soil profile, with the exception being for the A and AB horizons, which had a clay loam texture. The Pedon 3 typically maintained a consistent clay texture

Table 3
Physico-chemical properties of the investigated soils.

Soil types	Layers	Depth	pH	SOC	N	C/N	AP	Echangeable Cations				BS	CEC	Sand	Silt	Clay
		(cm)		(%)			(mg/kg)	K^+	Na^+	Ca^{2+}	Mg^{2+}	(%)		(%)		
								(Cmol.kg^{-1}soil)				(Cmol.kg^{-1}soil)				
	A	0–30	6.0	6.8	0.2	34.0	15.2	1.0	0.0	4.3	2.4	61.0	12.8	43.3	32.5	24.5
	Bw	30–70	6.7	1.1	0.1	11.0	9.4	0.6	0.0	4.5	2.9	59.9	13.3	54.0	31.8	14.3
	C	70–100	6.7	0.8	0.1	8.0	7.8	0.5	0.0	3.5	2.6	58.4	11.4	55.0	32.5	12.5
	AC	100–130	6.8	1.6	0.1	16.0	10.0	0.7	0.0	2.6	1.4	56.6	11.3	44.3	41.0	14.8
Pedon 1	2Bw	130–150	6.9	3.5	0.1	35.0	6.7	1.0	0.0	4.8	3.0	53.6	16.5	42.8	44.3	13.0
	A	0–20	4.9	4.1	0.1	41.0	12.6	0.4	0.0	4.4	1.2	21.3	10.5	57.0	19.3	23.8
	AB	20–80	5.0	2.4	0.1	24.0	19.1	0.3	0.0	1.9	0.2	20.8	11.6	33.0	30.0	37.5
	B1	80–100	5.1	2.7	0.1	27.0	8.4	0.3	0.0	4.8	1.6	25.1	13.5	33.5	19.3	47.3
Pedon 2	B2	100–150	5.9	1.7	0.1	17.0	6.6	0.3	0.0	3.5	1.0	20.5	9.6	28.3	24.0	47.8
	A	0–10	4.1	2.5	0.1	25.0	6.0	1.0	0.0	3.0	1.0	22.9	11.5	23.8	35.0	41.3
	AB	10–30	4.3	1.8	0.1	18.0	4.8	0.4	0.0	1.2	1.0	28.2	9.3	10.3	33.5	56.3
Pedon 3	B	30–150	5.2	1.6	0.1	16.0	4.6	0.4	0.0	2.6	1.6	24.6	13.2	8.3	24.5	67.3

L = Layer; SOC = Soil organic carbon; N = Nitrogen; C/N = carbon to Nitrogen ratio; AP = Available Phosphorus; BS = Base Saturation; CEC = Cation Exchange Capacity.

Table 4
Distribution of soil mineralogy in studied soils.

Soil type	Layers	BD	Cstock	Fed	Ald	Feo	Alo	Fep	Alp	Alo + 1/2Feo	Alo-Alp	Feo-Fep	Alp/Alo	Feo/Fed	Kaol	Go
			Kg/ha	%											%	
	A	0.73	14.89	13.54	2.94	0.94	2.55	0.20	1.93	3.02	0.62	0.74	0.76	0.07	–	–
	Bw	0.77	3.40	11.10	1.03	0.68	1.88	0.18	1.23	2.22	0.65	0.50	0.66	0.06	–	–
Pedon 1	C	0.85	2.04	10.76	1.00	0.46	0.87	0.11	0.70	1.10	0.17	0.35	0.81	0.04	–	–
	AC	0.79	3.79	11.11	0.65	0.57	0.85	0.09	0.54	1.14	0.31	0.48	0.63	0.05	–	–
	2Bw	0.78	5.46	12.70	1.30	0.62	2.15	0.10	1.00	2.46	1.15	0.52	0.47	0.05	–	–
Total Pedon 1	–	–	**29.58**	–	–	–	–	–	–	–	–	–	–	–	–	–
	A	0.80	6.56	9.71	2.04	0.27	1.92	0.04	0.78	2.06	1.15	0.24	0.40	0.03	76.5	23.6
Pedon 2	AB	0.84	4.03	7.34	0.90	0.11	0.49	0.01	0.35	0.54	0.14	0.10	0.71	0.01	86.2	13.8
	B1	0.99	5.34	7.68	0.81	0.07	0.45	0.02	0.30	0.48	0.15	0.05	0.67	0.01	83.3	16.7
	B2	1.02	8.67	6.71	0.63	0.05	0.37	0.01	0.28	0.39	0.09	0.04	0.77	0.01	68.4	31.6
Total Pedon 2	–	–	**24.6**	–	–	–	–	–	–	–	–	–	–	–	–	–
	A	1.07	2.68	7.22	1.61	0.23	0.34	0.07	0.00	0.46	0.34	0.16	0.01	0.03	64.1	35.9
Pedon 3	AB	1.10	3.96	6.77	0.62	0.05	0.31	0.01	0.01	0.34	0.31	0.05	0.02	0.01	71.0	28.9
	B	1.14	21.88	6.21	0.73	0.02	0.20	0.00	0.00	0.21	0.20	0.02	0.02	0.00	71.3	28.7
Total in Pedon 3	–	–	**28.52**	–	–	–	–	–	–	–	–	–	–	–	–	–

L = Layer; BD = Bulk Density; Fed, Ald = Dithionite-citrate extractable Al and Fe; Fep, Alp = Pyrophosphate extractable Al, Fe; Feo, Alo = Acid oxalate extractable Al, Fe; Alo -Alp and Feo-Fep are derived predominantly from short-range-order minerals; Feo/Fed is an index of Fe (hydr)oxide activity. Alp/Alo indicates organo-Al contribution to active Al fraction; Kaol = Kaolinite; Gib = Gibbsite; Go = Goethite; EG = Ethylene Glycol; C-stock = Carbone stock.

throughout the entire soil profile. The porosity varied from high in Pedon 1 profile to moderate in Pedon profile 2 and low in Pedon 3 profile. The rooting patterns shifted from deep in the Pedon 1 profile to shallow in the Pedon 2 and Pedon 3. There was no evidence of water stagnation in any of the soils investigated (Fig. 2).

The morphology of Pedon 1 in the highland shows dark (2.5Y and 10YR) multi-sequum horizons due to intermittent tephra deposition, with granular structures and a loamy texture. In contrast, the morphology of Pedon 2 exposes distinctive horizons characterized by a dark (10YR) surface soil and a brown (7.5YR) subsurface soils, showing an angular to sub-angular blocky structure and clay loam to clay texture. Additionally, the morphology of Pedon 3 exhibits a distinct horizon with a brown (2.5YR) color, a dominant massive structure, and clay texture throughout its profile.

3.2. Basic physical and chemical properties

The Pedon 1 profile was slightly acidic to neutral (6.0–6.9), the Pedon 2 was slightly acidic (4.9–5.9) and the Pedon 3 was acidic (4.1–5.2) (Table 2, Fig. 3A). The variation of SOC content ranged between 0.8 and 6.8 % in P1 profile, 1.7–4.1 % in P2 and 1.6–2.5 % in P3 (Table 3,). The lowest value of SOC was found in the deepest layer and the highest value of SOC was reported in the surface horizon of all soil profiles. The nitrogen (N) value was 0.1 % in all soil profiles. The C/N ratio had the highest value in the surface horizon for Pedon 1 profile (34.0), Pedon 2 (41.0) and Pedon 3 (25.0) (Table 3). Pedon 1 profile had the highest available content (AP) (15.2 mg/kg) in horizon A, which decreased with depth. Similarly, Pedon 2 had the highest AP content (19.1 mg/kg) in the AB horizon, while B1 and B2 horizon had the lowest values (8.4 and 6.6 mg/kg, respectively). For the Pedon 3, the surface horizon had the highest AP content (6.0 mg/kg), which decreased with depth. In the Pedon 1 profile, calcium (Ca^{2+}) concentrations ranged from 2.6 to 4.8 cmol.kg-1 soil (lowest in AC horizon, highest in 2Bw), while Pedon 2 showed 1.9 cmol.kg-1 in the AB horizon and 4.8 cmol.kg-1 in the B1 horizon, and Pedon 3 had the highest concentration of 3.0 cmol.kg-1 in the surface horizon and the lowest in the AB horizon. The base saturation (BS) variation was 53.6–61.0 % in Pedon 1, 20.5–21.3 % in Pedon 2 and 22.9–28.2 % in Pedon 3. These BS values decreased from Pedon 1 to Pedon 3, with decreasing elevation. The CEC was low in all the Pedon with the value being less than 20 $cmol.kg^{-1}$soil (Table 3). The content of sand in Pedon decreased gradually with decreasing elevation. The clay content increased with decreasing elevation (Table 3, Fig. 3C).

3.3. Selective dissolution analysis

Figs. 3 (E and F) presented the data obtained from bulk density (BD) and selective dissolution analysis. The bulk density varied between 0.73 and 0.85 g/cm^3 in Pedon 1, 0.80–1.02 g/cm^3 in Pedon 2 and 1.07–1.14 g/cm^3 in Pedon 3. The findings indicated a decrease in Fed with increasing soil depth in all soil profiles, except for Pedon 1. With respect to Fed concentration, Pedon 1 profile recorded the highest values (10.76–13.54 %), followed by Pedon 2 (6.71–9.71 %), and Pedon 3 (6.21–7.22 %). Similarly, the concentration of Ald showed a similar trend across all soil profiles, with higher levels observed in Pedon 1 profile (0.65–2.94 %) than in Pedon 2 (0.63–2.04 %) and Pedon 3 (0.62–1.61 %). Notably, the concentration of Ald exceeded 1 % only in A horizon of Pedon 2 and Pedon 3.

Across all soil profiles, Feo concentrations were less than 1 in all layers. Meanwhile, Alo concentrations, which were highest in Pedon 1 profile (0.85–2.55 %), declined with increasing soil depth in all soils, exhibiting lower values in Pedon 2 (0.45–1.92 %) and Pedon 3 (0.20–0.34 %). Similarly, Fep concentrations were below 1 % in all soils. Regarding Alp, its concentrations were also less than 1 % in all soils except Pedon 1 profile where the highest concentration (1.93 %) was observed in A horizon, while the lowest concentration was recorded in AC horizon (Table 4).

The concentration of Alo + 1/2Feo in Pedon 1 profile exceeded the minimum required for andic soil properties (2 %) in A, Bw, and 2Bw horizons, and was less than 2 % in other horizons. Furthermore, this value decreased with increasing soil depth. In Pedon 2 profile, the Alo + 1/2Feo percentage was approximately 2 % in A horizon, while it was less than 1 % in all the other horizons. Especially, the concentrations of Alo + 1/2Feo were less than 1 % in all the horizons of Pedon 3 (Table 3, Fig. 3E). The concentrations of Alo – Alp declined with decreasing depth in all soils and presented a great concentration in Pedon 1 profile compared to Pedon 2 and Pedon 3. Moving on to Feo-Fep concentrations, it was higher in Pedon 1 profile (0.35–0.74 %) in comparison to Pedon 2 (0.04–0.24 %) and Pedon 3 (0.02–0.16 %). Particularly, these concentrations showed a decreasing trend with decreasing soil depth. The percentage of Alp/Alo ratio was around 1 % in Pedon 1 profile and Pedon 2 compared to Pedon 3, where these values were less than 0.1 %. The concentrations of Feo/Fed were less than 0.1 % in all soils (Table 4).

The carbon stock (C-stock) varies significantly across the three Pedons and their respective horizons (Table 3, Fig. 3F). Pedon 1 exhibits a high C-stock in the A horizon (14.89 kg/ha) and shows a notable decrease in the Bw and C horizons (3.40 kg/ha and 2.04 kg/ha,

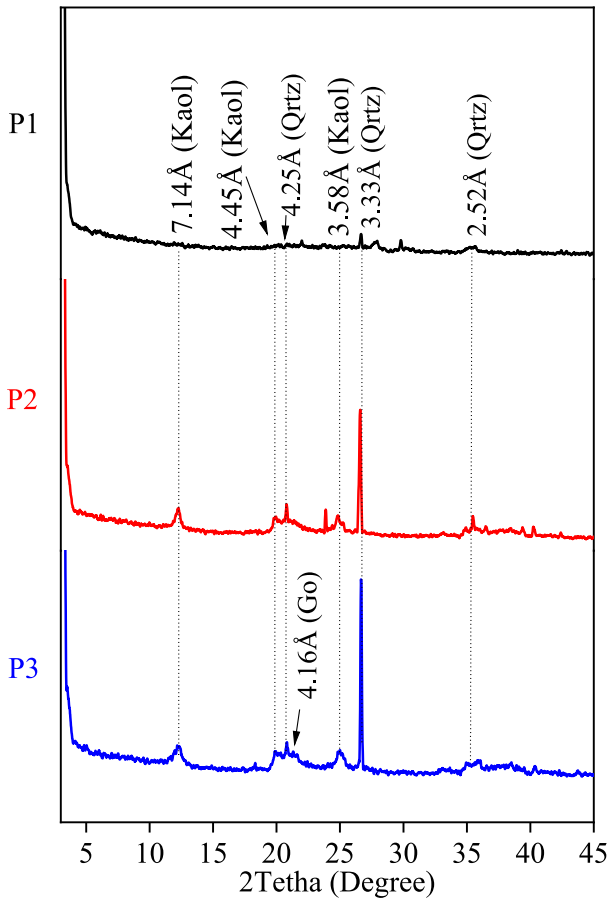

Fig. 4. X-ray diffractograms of powder bulk samples from topsoil horizons. Kaol = Kaolinite; Gib = Gibbsite; Qtrz = Quartz

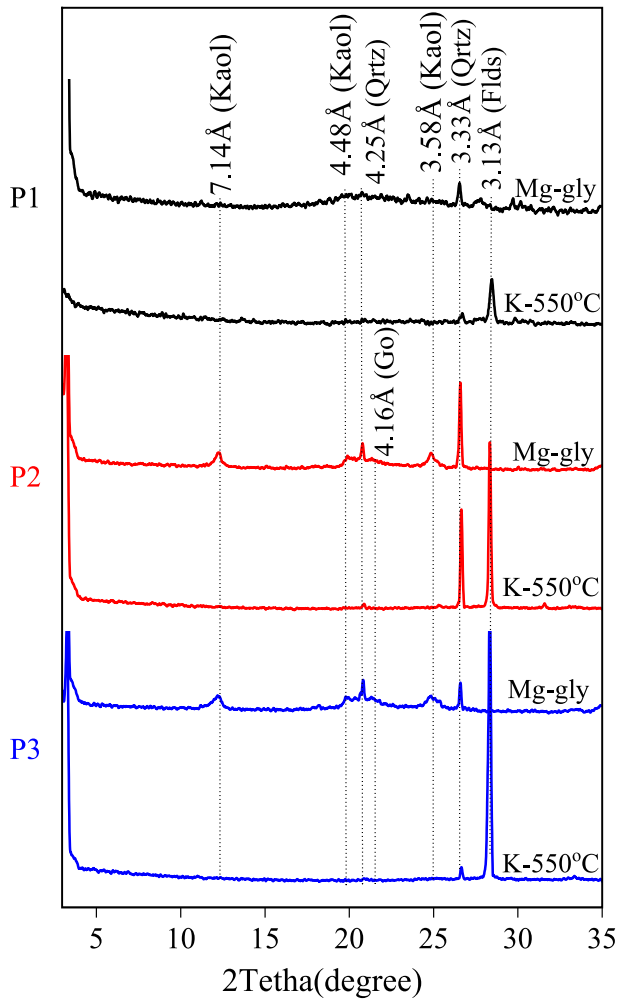

Fig. 5. X-ray diffractograms of oriented clay fraction samples from topsoil horizons. Treatments: Mg-gly = Mg saturated and ethylene glycol-solvated, K-550 °C = K-saturated and heated to 550 °C.

respectively). The C-stocks in Pedon 2 varied from 6.56 kg/ha in A horizon to 4.03 kg/ha and 5.35 kg/ha in B1 and B2, respectively. Pedon 3 presents C-stock contents, with 2.68 kg/ha in A horizon, 3.96 kg/ha in the AB horizon, and 21.88 in B horizon, probably because the B horizon is deeper than the surface horizon.

3.4. X-ray diffraction and Fourier-transform infrared spectroscopy analysis

X-ray diffractograms were displayed in Figs. 4 and 5 (Topsoils), and the clay minerals composition in Table 4 (all the horizons) while the FTIR spectra were reported in Fig. 6.

Kaolinite and goethite were crystalline minerals while the allophane and ferrihydrite are the dominant short-range ordered minerals in the studied soils (Table 4). The presence of kaolinite was identified in the diffractogram by the reflection peaks at 7.14, 4.45 and 3.58 Å, which disappeared after heating the K-saturated samples at 550 °C (Figs. 4 and 5) (Ndzana et al., 2018). The goethite was identified by the presence of reflection peaks at 4.16 Å (Ahanda et al., 2019). The presence of SRO was indicated by the absence of reflection peaks on the X-ray diffractogram under conventional XRD analysis and the poor crystallinity of clay minerals in certain soils (Figs. 4 and 5, Table 5).

In the Pedon 1 profile of this study, kaolinite and goethite were not observed in the X-ray diffractogram, only short-range ordered minerals (SRO) such as allophane and ferrihydrite were detected (Figs. 4 and 5). The distribution of SRO revealed that both allophane and ferrihydrite concentrations were highest at the surface layers and decreased gradually with depth. Additionally, the Pedon 1 profile demonstrated a higher concentration of allophane compared to ferrihydrite (as shown in Table 4).

In Pedon 2, there was a mixture of crystalline and SRO minerals. The crystalline minerals were dominated by kaolinite and goethite (Figs. 4 and 5). The concentration of kaolinite varied between 68.4 and 86.2 %, with the lowest value in the B2 horizon and the highest value in AB horizon (Table 3). The concentration of goethite varied from 13.8 % to 31.6 %, with the maximum in AB horizon and the maximum in B2 horizon. The SRO minerals were dominated by allophane (1.9–5.0 %), follows by ferrihydrite (0.8–1.6 %). These SRO minerals were more concentrated at the surface layers (Table 4). However, it is important to note that it was not possible to detect clay minerals in Pedon 1 using the conventional XRD analysis since most of the clay minerals in this soil are poor crystalline structure(Ndzana et al., 2019).

The Pedon 3 was dominated by kaolinite (64.1–71.3 %), followed by goethite (28.7–35.9 %) (Table 4). The kaolinite and goethite declined with depth.

To evaluate the degree of crystallinity of kaolinite of P2 and P3, the peak height/area ratio, and their full width at half maximum height of diffraction peak (FWHM) were calculated. The mineral with lowest Peak height/Area ratio and highest FWHM presented the poorest crystalline structure (Burnett, 1995; Ndzana et al., 2022; Zhang et al., 2017). The properties of kaolinite at the surface horizon of Pedon 2 and Pedon 3 showed a peak height/area ratio of 0.01 and 0.02, respectively while the full width at half maximum (FWHM) was 0.60 and 0.55 degree, respectively (Table 6). This indicates that kaolinite in P2 presented the

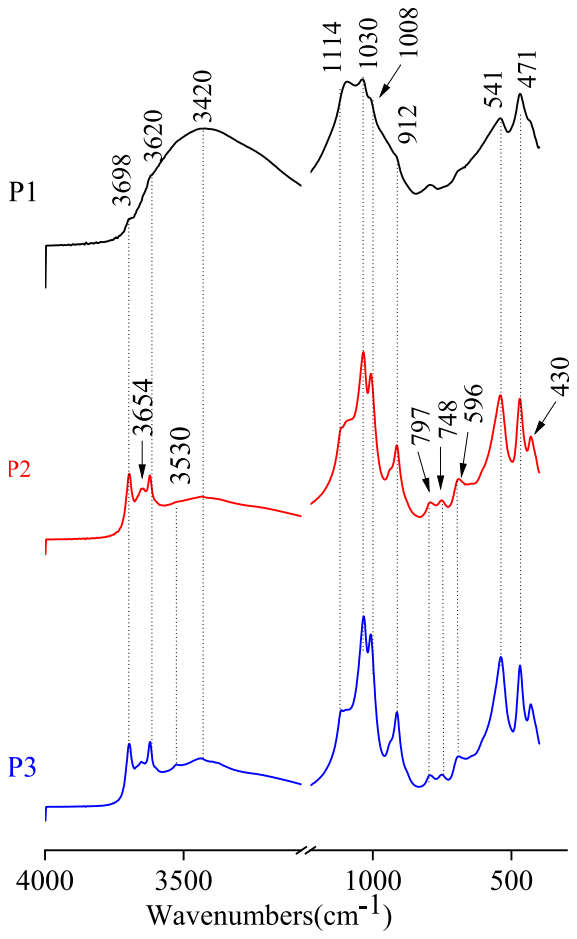

Fig. 6. Fourier-Transform Infrared (FTIR) spectra of studied soil samples from topsoil horizons, with the bands between 4000 and 400 cm^{-1}.

Table 5
Short-range-order secondary phases in soils with andic properties.

Soil type	Layers	Si_o	Allophane	Ferrihydrite	(Alo-Alp) /Sio
	(Cm)	(%)	(%)		
Pedon 1	A	0.70	4.97	1.60	0.89
	Bw	0.51	3.62	1.16	1.27
	C	0.28	1.99	0.78	0.61
	AC	0.31	2.20	0.97	1.00
	2Bw	0.55	3.91	1.05	2.09
Pedon 2	A	0.63	4.40	0.46	1.84
	AB	0.48	3.41	0.19	0.29
	B1	0.15	1.07	0.12	1.00
	B2	0.19	1.35	0.09	0.47

Table 6
Crystalline structure of kaolinite in different Oxisol of the study area.

Soil types	Clay Minerals	Peak Height	Area (Count)	Peak height/ Area ratio	FWHM (°)
P1	–	–	–	–	–
P2	Kaolinite	95	5139	0.01	0.60
P3	Kaolinite	65	3243	0.02	0.55

FWHM: Full Width at Half Maximum; P1: Pedon 1; P2: Pedon 2; P3: Pedon 3.

poorest crystalline structure compared to kaolinite in P3.

The results of FTIR spectroscopy of surface horizons (bulk soil) were displayed in Fig.6. In the range 2800–3600 cm^{-1}, distinctive bands appeared in all soils indicating the O—H stretching. The presence of four bands (3530, 3620, 3654 and 3698 cm^{-1}) between 3500 and 3700 cm^{-1} wavenumbers confirmed the existence of kaolinite mineral in both Pedon 2 and Pedon 3 (Madejová, 2003). These bands corresponded to structural hydroxyl (-OH) groups, O—H stretching of inner hydroxyl groups, stretching vibrations of the hydroxyl (-OH) groups and out-of-plane stretching vibrations of surface hydroxyl groups, respectively (Candra et al., 2023; Madejová, 2003). Moreover, the fingerprint of kaolinite bands was also revealed at 912 cm^{-1} (inner hydroxyl groups), 1008–1030 cm^{-1} (O—H angular deformation and Si—O axial deformation)(Candra et al., 2023; Madejová, 2003; Merlin et al., 2014). The double bands 1008–1030 cm^{-1} was also used as indicator of kaolinite in the Pedon 2 and Pedon 3 (Hong et al., 2018).

4. Discussion

4.1. Morphological features and physical characteristics

The Pedon of this study exhibited significant differences in key morphological properties of horizons across both varying altitudes and climate gradient, highlighting the interaction between vertical variability within the soil profile and distinct soil-forming factors. Color is a key indicator of many soil properties and contributes to soil classification. With decreasing altitude and climate gradient, the colors of the Pedon profiles exhibit a shift from dark color (2.5Y and 10YR) in Pedon 1 to brown color (7.5 YR) in Pedon 2 and reddish color (2.5YR) in Pedon 3 with the exception being for the surface horizon of Pedon 2, which retains a dark color (10YR). In this study, the dark color in the surface horizon of Pedon 1 and Pedon 2 agreed with the previous studies (Khan and Fenton, 1994; Łabaz et al., 2019; Nizeyimana, 1997) and was attributed to the higher amount of organic matter (Liles et al., 2013). However, the Bw, and AC horizons had dark colors while the soil organic carbon content was low compared to other horizons. This darkness could be attributed to the presence of dark pozzolan (volcanic materials derived from volcanic activities) granules dispersed throughout the subsoil horizons of the profile. The natural pozzolan was reported to have dark brown/blackish color (Dedeloudis et al., 2018). It is important to note that pozzolan materials can vary in color; they are not limited to dark hues. Some pozzolans may be light in color (McCarthy and Dyer, 2019), which could influence the overall appearance of the soil profile. The variation in pozzolan color suggests that while the dark granules may contribute to the observed darkness in certain horizons, the intrinsic characteristics of the pozzolan itself must also be considered. The brown color (7.5 and 2.5 YR) found in Pedon 2 and the red color in Pedon 3 are very common in tropical soils and were mainly due to the presence of mineral like goethite and hematite, respectively (Bigham et al., 1978; Fontes and Carvalho Jr, 2005; Torrent et al., 1983).

The granular structure observed in Pedon 1 was mainly reported in volcanic ash soils (Hewitt et al., 2021; Shoji et al., 1993). The granular structure of volcanic soils can be attributed to several interrelated factors. The mineralogical composition, including amorphous minerals such as allophane and imogolite, is a key factor in the formation of granules. These minerals are highly reactive and can create stable aggregates by bonding with other soil particles (Hewitt et al., 2021; Stoops et al., 2018). The granular structure of the Pedons of this study could be attributed to the amorphous mineral reported in this study.

One possible explanation for the development of angular blocky structures in Pedon 2 could be the alternation of drying and wetting cycles, which can create tensile and shear fractures (cracks) in the soil (Camacho et al., 2021). These fractures can break up the soil mass into aggregates, resulting in the blocky structure observed (Horton et al., 2016).

When comparing the morphology of the three Pedons with decreasing elevation and climatic gradient, it appeared that the Pedon 1 located at a high altitude with tropical highland climate was characterized by the development of soil horizons with varying degrees of

weathering, leading to the formation of a multi-sequum profile. At the intermediate elevation, where the climate transitions from tropical rainforest to tropical highland, Pedon 2 exhibited a brown soil profile characterized by a black surface horizon. The profile 2 at the intermediate elevation is not common in the tropical soils and was mainly reported in the soils under volcanic materials, highlighting the key role of volcanic material during the soil formation process, in agreement with previous studies (Candra et al., 2023; Gavenda, 1989; Simmons, 1990). In this study, the similarities in mineralogy of the two surface horizons (Pedon 1 and Pedon 2), confirm the influence of volcanic ash materials in the black surface horizon formation. Moreover, our study indicated that Pedon 1, characterized by a deep, dark surface horizon exceeding 25 cm in depth and exhibiting the highest soil organic carbon (SOC) content, aligns with the characteristics of black soils as documented by the INBS-ITPS (FAO, 2019).

4.2. Mineralogy and chemical properties of Pedons

With the decreasing altitude and climatic gradient, the Pedons of this study showed mineralogical and chemical properties marked changes. For instance, SOC content in surface horizons of Pedon decreased from 6.8 to 2.5 % with decreasing altitude and climatic gradient (Table 3 and Fig. 3B). This trend of SOC content indicated that the accumulation and stabilization of SOC occurred in highland compared to lowlands, in agreement with the studies reported previously (Candra et al., 2023; Gerzabek et al., 2022; Tsozué et al., 2019). These authors argued that the stabilization of SOC was due to SRO mineral phases abundance. Indeed, short-range order (SRO) minerals, such as allophane, imogolite, and ferrihydrite, play a pivotal role in stabilizing SOC through several mechanisms. Firstly, SRO minerals have high surface area and reactive sites, which enhance their ability to adsorb and bind organic molecules (Chatterjee et al., 2022; Matus et al., 2014). Additionally, their amorphous nature allows for the formation of organo-mineral complexes, where organic carbon is physically and chemically stabilized within the soil matrix, leading to the protection of SOC from microbial degradation (Tamrat et al., 2019; Xiao et al., 2016). Additionally, the observed decrease in soil organic carbon (SOC) content with decreasing altitude and changing climatic gradients can also be explained through a combination of pedogenic factors. At higher elevations, the cooler temperatures create conditions that slow microbial activity, reducing decomposition rates and allowing for greater retention of organic carbon within the soil (Hobbie et al., 2000; Wagai et al., 2013). Conversely, as altitude decreases and the climate transitions to warmer conditions, microbial activity tends to increase, leading to more rapid decomposition of organic matter, which consequently results in lower SOC levels (Nottingham et al., 2015; Zhang et al., 2023). In our study SRO minerals were identified in the highlands and middle lands surface horizon compared to lowlands surface horizon where kaolinite, and goethite are dominant minerals (Tables 4 and 5). Additionally, the annual temperature decreases from cooler (15 °C) in highlands to warmer (27 °C) in lowland and annual precipitation decreases from 2500 to 2000 mm from highland to lowland. These SRO minerals and pedogenetic factors (elevation and climate) could be the potential drivers of SOC accumulation and stabilization in the highland and middle land surface horizon.

We observed a decline in pH levels in the surface horizon of Pedons as altitude and climate change from highland to lowland. Specifically, pH level in the surface horizon decreased from 6.0 in Pedon 1 to 4.9 in Pedon 2, and further to 2.5 in Pedon 3 (Table 3, Fig.3A). Similar results of pH were reported with decreasing hydroclimatic gradient in Santa Cruz Island and in Hawaiian (Candra et al., 2023; Chadwick et al., 2003).

The surface horizon clay contents of various Pedons of this study showed a consistent altitudinal trend, increased with decreasing elevation (Fig. 3C). Indeed, the clay content varied from 24.5 % in the surface horizon of highland to 41,3 % in the surface horizon of lowland (Table 3 and Fig. 3C). The lower clay content in the surface horizon of highlands is likely a result of clay migration. During the process of soil formation, erosion may have facilitated the movement of clay particles from the highlands towards the surface horizons of lowland areas (Winkler et al., 2016).

The clay mineralogy of this study (Figs. 4 and 5) showed a pronounced altitudinal change, shifting from SRO minerals (allophane, ferrihydrite) in the highland surface horizon to poor crystalline kaolinite in the middle land to well crystalized kaolinite in lowland (Tables 4, 5 and 6). This clay minerals sequence highlights the relationship between soil formation processes and environmental factors (climate, elevation, and parent materials). At higher elevations, the predominance of short-range order (SRO) minerals such as allophane and ferrihydrite was in agreement with previous studies (Chadwick et al., 2003; Rasmussen et al., 2007; Zehetner et al., 2003) and suggests conditions characterized by the influence of climate conditions and volcanic materials, which are often rich in amorphous silicate minerals (Nanzyo, 2002; Parfitt, 2009). These SRO minerals are commonly associated with volcanic ash soils and typically formed under conditions which are prevalent in cooler highland environments. As altitude decreases, the shift towards poorly crystalline kaolinite in the middle elevations indicates a transition to warmer temperatures and altered precipitation regimes, which promote more intensive weathering and the formation of crystalline clay minerals (Lyu et al., 2022; Tsai et al., 2010). In the lowland areas, the presence of well-crystallized kaolinite signifies a stabilization of soil conditions, where prolonged weathering has favored the transformation of less stable minerals into more thermodynamically favored forms (Churchman and Lowe, 2012; Manju, 2002).

4.3. Soil classification along the altitude and climate gradient

The classification of soils along the studied toposequence reflects significant variations in morphological and pedogenic characteristics, highlighting the influence of environmental factors on soil development. Pedon 1 exhibits distinct andic properties demonstrated by its low bulk density and high Alo + ½Feo values. Similar properties were observed by Watanabe et al. (2023) in volcanic soils of Cameroon and Takahashi and Shoji, (2002) in volcanic soils of Japan. These soils are classified as Mollic Vytric Silandic **Andosol** (Loamic, Eutrosilic, Humic) according to the WRB soil classification system (IUSS Working Group WRB, 2022). The presence of volcanic glass, specifically pozzolan granules, further supports the classification due to their role in enhancing soil structure and fertility (El-Desoky and Hafez, 2018).

In contrast, Pedon 2 is regarded as a Dystric Xanthic **Andic Ferralsol** (Clayic, Humic) due to its ferralic horizon characterized by low-activity clays and resistant minerals as well as its high organic carbon content at the surface horizon which further corroborates this classification, highlighting the interplay between organic matter and mineralogy. The Andic Ferralsol where reported to be dominant in the middle land of Bamboutos mountain in Volcanic Line of Cameroon (Temgoua et al., 2014).

The classification of Pedon 3 as an Umbric Rhodic **Ferralsol** (Clayic, Humic) indicates a shift towards a more leached profile, characterized by umbric properties with a distinct lack of andic qualities. The dominance of kaolinite and low organic matter suggests significant weathering processes consistent with soils formed in more humid conditions (Vieira et al., 2025).

4.4. Soil organic carbon stock and degradation potential risks of studied soils

Beside the WRB classification system, the comparison of the colors and the soil organic matter contents of the three Pedons indicates that Pedon 1 fits the concept of Black Soils from INBS / ITPS-FAO and it is therefore considered as a tropical Black Soil compared to the Pedon 2 and Pedon 3 (FAO, 2019). Black soils are considered as key sources for food productivity and climate change mitigation because of their carbon

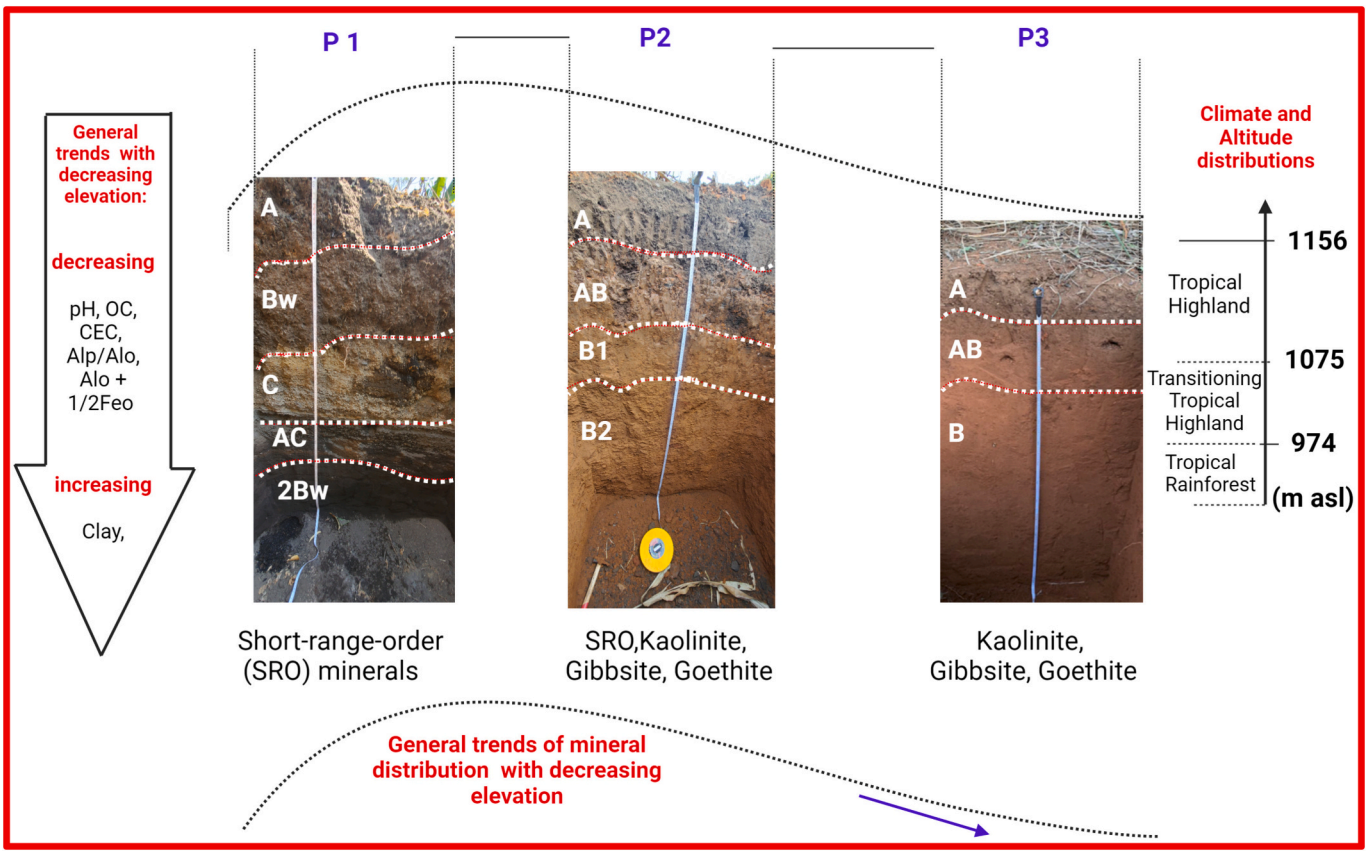

Fig. 7. Conceptual summary of mineralogical changes and pedogenesis of soils along the studied elevation sequence of Foumbot, West Cameroon. Alo and Feo = oxalate-extractable Al and Fe; Alp = pyrophosphate-extractable Al; CEC = cation exchange capacity, OC = Organic Carbon.

stock capacity (Krasilnikov et al., 2022). In this study, the variation of soil organic carbon stock in the top 30 cm of the Pedon 1 highlights the greater potential of black Andosol soils to effectively sequester carbon, compared to other soil types.

However, black soils are increasingly under threat because of the long-standing and intensive cultivation, land use change, unsustainable management, and agrochemical overuse have led to significant degradation, including SOC loss, erosion, acidification, nutrient depletion, and biodiversity decline (Tong and Sorokin, 2024). In this study, the three soils are intensively cultivated and thus exposed to severe degradation. However, andosol black soils, because of their specific properties including high sand contents (inducing friable macrostructure), low bulk density, and their position at the top of hill, are more susceptible for erosion compared to other soils. Previous studies reported the fragile status of andosol and their sensitivity to erosion (Avilés-Junco et al., 2025; Kome et al., 2018; Tematio et al., 2011). The mixture factors including intensive agriculture, poor farming practices and high rainfall are the main cause of soils erosion in the study area (Inyang, 2011; Ngandeu-Mboyo et al., 2016).

5. Summary and conclusion

The present study aimed to investigate the morphology, physical and chemical properties, and mineralogy of soils within the climotoposequence of Foumbot with the intension to evaluated the potential risks of soil degradation in this region. A conceptual summary of the main results of this study is shown in Fig. 7. The three Pedons, which represent the predominant soil types in this area, exhibit significant variation in their morphology, physical characteristics, chemical properties, and mineralogical composition. This diversity has contributed to the formation of different soil types within the climotoposequence of Foumbot. Pedon 1, located in the highlands, was classified as Mollic *Vitric* Silandic **Andosol** (Loamic, Eutrosilic, Humic), Pedon 2, located in the intermediary land, as Dystric Xanthic Andic **Ferralsol** (Clayic, Humic), and Pedon 3 situated in the lowland as Umbric Rhodic **Ferralsol** (Clayic, Humic), according to the WRB classification. Moreover, pedon 1, which was classified as andosol, presents characteristics that fit the definition of black soil according to the INBS-FAO definition. This soil shows greater potential for agricultural productivity and carbon storage compared to the other two Pedons. However, since these andosols are situated at the top of the hill, possess structural weaknesses (granular structure), and are subjected to intensive cultivation, they pose a higher potential risk of degradation when farming is practiced compared to the other two Pedons. Consequently, this area necessitates additional research aimed at identifying the land use practices and management systems impacting andosols and ferralsols. Such studies will help develop innovative strategies for the sustainable management of these soil types in the region.

CRediT authorship contribution statement

Georges Martial Ndzana: Methodology, Funding acquisition, Formal analysis, Data curation, Conceptualization. **Jeroen Meersmans:** Methodology, Funding acquisition, Conceptualization. **Li Huang:** Data curation, Conceptualization. **Tabi Fritz Oben:** Conceptualization. **Etienne Mboua:** Conceptualization. **Azinwi Primus:** Methodology. **C.T. Kaamil Fonfatawouo:** Formal analysis. **Danielle Mamba:** Methodology. **Etienne Bekoa:** Formal analysis. **Bertrand Mungu Akam:** Formal analysis. **Joseph Kabala Mubolo:** Methodology. **Bin Zhang:** Methodology, Investigation.

Declaration of competing interest

The authors declare that they have no known competing financial interests or personal relationships that could have appeared to influence the work reported in this paper.

Acknowledgment

This study was supported by the Academy of Research and Higher Education (ARES)-Belgium through the Black soil project 2023-2025 and by the Modernization Grant 2023-2024 for University Research in Cameroon. Thanks also to the handling editor, and two anonymous reviewers for their constructive inputs.

Data availability

Data will be made available on request.

References

Ahanda, D.H.O., Ndzana, G.M., Bekoa, E., Abane, M.A.-A., Bitom, L.D., 2019. Morphological, geochemical and mineralogical studies of two soil profiles developed on the itabirites of Ntem Complex, southern Cameroon. J. Afr. Earth Sci. 153, 111–129.

Anwar, U., 2014. Soil Moisture Patterns and Hydraulic Properties Associated with Alternative Biomass Cropping Systems across a Landscape Gradient.

Avilés-Junco, C., Prado-Pano, B., Mora-Palomino, L., Velázquez, A., Abbruzzini, T.F., Siebe, C., 2025. Integrated multiscale assessment of andosol degradation after conversion from grasslands to agriculture. Catena 250, 108731.

Batjes, N.H., 1996. Total carbon and nitrogen in the soils of the world. Eur. J. Soil Sci. 47 (2), 151–163.

Bernasconi, S.M., Bauder, A., Bourdon, B., Brunner, I., Bünemann, E., Chris, I., Derungs, N., Edwards, P., Farinotti, D., Frey, B., 2011. Chemical and biological gradients along the Damma glacier soil chronosequence, Switzerland. Vadose Zone J. 10, 867–883.

Bidias, L.A.Z.A., Kameni, L.H.N., Moundi, A., Kamgang, P., 2023. Geoheritage of the volcanic landscapes of Foumbot-Kouomboum region, Noun Plain, Cameroon: geomorphological features and assessment of geomorphosites. Int. J. Geoheritage Parks 11 (3), 464–482.

Bigham, J., Golden, D., Buol, S., Weed, S., Bowen, L., 1978. Iron oxide mineralogy of well-drained ultisols and oxisols: II. Influence on color, surface area, and phosphate retention. Soil Sci. Soc. Am. J. 42, 825–830.

Blake, G., 1965. Bulk density. Methods of soil analysis: part 1 physical and mineralogical properties, including statistics of measurement and sampling, 9, 374–390.

Bojko, O., Kabala, C., 2016. Transformation of physicochemical soil properties along a mountain slope due to land management and climate changes—a case study from the Karkonosze Mountains, SW Poland. Catena 140, 43–54.

Burnett, A.D., 1995. A quantitative X-ray diffraction technique for analyzing sedimentary rocks and soils. J. Test. Eval. 23, 111–118.

Camacho, M.E., Mata, R., Barrantes-Víquez, M., Alvarado, A., 2021. Morphology and characteristics of eight Oxisols in contrasting landscapes of Costa Rica. Catena 197, 104992.

Candra, I.N., Gerzabek, M.H., Ottner, F., Wriessnig, K., Tintner, J., Schmidt, G., Rampazzo, N., Zehetner, F., 2023. Soil formation and mineralogical changes on basaltic lava vs scoria along a hydroclimatic gradient on Santa Cruz Island, Galápagos. Catena 220, 106696.

Chadwick, O.A., Gavenda, R.T., Kelly, E.F., Ziegler, K., Olson, C.G., Elliott, W.C., Hendricks, D.M., 2003. The impact of climate on the biogeochemical functioning of volcanic soils. Chem. Geol. 202, 195–223.

Chatterjee, D., Datta, S., Manjaiah, K., Mandal, N., 2022. Short-range order (SRO) minerals and their implications in sustainable agriculture by exerting influence on carbon sequestration and fixation of phosphorus and potassium. In: Soil Management for Sustainable Agriculture. Apple Academic Press, pp. 73–97.

Childs, C.W., Wells, N., Downes, C.J., 1986. Kokowai Springs, Mount Egmont, New Zealand: chemistry and mineralogy of the ochre (ferrihydrite) deposit and analysis of the waters. J. R. Soc. N. Z. 16 (1), 85–99.

Churchman, G.J., Lowe, D.J., 2012. Alteration, Formation, and Occurrence of Minerals in Soils. CRC press.

Crews, T.E., Kitayama, K., Fownes, J.H., Riley, R.H., Herbert, D.A., Mueller-Dombois, D., Vitousek, P.M., 1995. Changes in soil phosphorus fractions and ecosystem dynamics across a long chronosequence in Hawaii. Ecology 76, 1407–1424.

Daily, G.C., Matson, P.A., Vitousek, P.M., 1997. Ecosystem services supplied by soil. Nat. Serv. 113–132.

Dedeloudis, C., Zervaki, M., Sideris, K., Juenger, M., Alderete, N., Kamali-Bernard, S., Villagrán, Y., Snellings, R., 2018. Natural pozzolans. Properties of Fresh and Hardened Concrete Containing Supplementary Cementitious Materials: State-of-the-Art Report of the RILEM Technical Committee 238-SCM, Working Group, 4, pp. 181–231.

Dessalegn, D., Beyene, S., Ram, N., Walley, F., Gala, T.S., 2014. Effects of topography and land use on soil characteristics along the toposequence of Ele watershed in southern Ethiopia. Catena 115, 47–54.

Dincă, L.C., Dincă, M., Vasile, D., Sparchez, G., Holonec, L., 2015. Calculating organic carbon stock from forest soils. Notulae Botanicae Horti Agrobotanici Cluj-Napoca 43 (2), 568–575.

Ehrlich, P.R., Ehrlich, A.H., Daily, G.C., 1993. Food security, population and environment. Population and development review, pp. 1–32.

El-Desoky, H.M., Hafez, H.M., 2018. Petrology, Geochemistry and Mineralogy of the Hydrothermally Altered Rock Units at Wadi Dara, North Eastern Desert, Egypt. Ann. Geol. Surv. Egypt 35, 103–140.

Enang, R.K., Yerima, B.P.K., Kome, G.K., Van Ranst, E., 2019. Short-range-order minerals and dominant accessory properties controlling P sorption in tropical tephra soils of the Cameroon volcanic line. Open J. Soil Sci. 9 (8), 113–139.

FAO, 2019. Black Soils Definition [online]. [cited 11 April 2025]. https://www.fao.org/global-soil-partnership/intergovernmental-technical-panel-soils/gsoc17-implementation/internationalnetworkblacksoils/more-on-black-soils/definition-what-is-a-black-soil/en/.

Fokeng, R.M., Fogwe, Z.N., Yemelong, N.T., 2020. Modelling alternatives for Highland soil structural degradation and erodibility, Bui Plateau, Cameroon. Eur. J. Environ. Earth Sci. 1.

Fontes, M.P., Carvalho Jr., I.A., 2005. Color attributes and mineralogical characteristics, evaluated by radiometry, of highly weathered tropical soils. Soil Sci. Soc. Am. J. 69, 1162–1172.

Gavenda, R.T., 1989. Soil Genesis and Landscape Evolution in Central Oahu, Hawaii.

Gerzabek, M.H., Rechberger, M.V., Schmidt, G., Wriessnig, K., Zehetner, F., 2022. Soil organic carbon and fine particle stocks along a volcanic chrono-and elevation-sequence on the Galápagos archipelago/Ecuador. Geoderma Reg. 29, e00508.

Ghani, M.I., Wang, J., Li, P., Pathan, S.I., Sial, T.A., Datta, R., Mokhtar, A., Ali, E.F., Rinklebe, J., Shaheen, S.M., 2023. Variations of soil organic carbon fractions in response to conservative vegetation successions on the Loess Plateau of China. Int. Soil Water Conserv. Res. 11, 561–571.

Gutiérrez-Girón, A., Díaz-Pinés, E., Rubio, A., Gavilán, R.G., 2015. Both altitude and vegetation affect temperature sensitivity of soil organic matter decomposition in Mediterranean high mountain soils. Geoderma 237, 1–8.

Hailemariam, M.B., Woldu, Z., Asfaw, Z., Lulekal, E., 2023. Impact of elevation change on the physicochemical properties of forest soil in south omo zone, southern Ethiopia. Appl. Environ. Soil Sci. 2023, 7305618.

Hartemink, A.E., Barrow, N., 2023. Soil pH-nutrient relationships: the diagram. Plant Soil 486, 209–215.

He, Y., Li, D., Velde, B., Yang, Y., Huang, C., Gong, Z., Zhang, G., 2008. Clay minerals in a soil chronosequence derived from basalt on Hainan Island, China and its implication for pedogenesis. Geoderma 148, 206–212.

Hewitt, A.E., Balks, M.R., Lowe, D.J., Hewitt, A.E., Balks, M.R., Lowe, D.J., 2021. Granular Soils. Soils Aotearoa New Zealand 87–100.

Hobbie, S.E., Schimel, J.P., Trumbore, S.E., Randerson, J.R., 2000. Controls over carbon storage and turnover in high-latitude soils. Glob. Chang. Biol. 6, 196–210.

Hong, Z.-N., Jiang, J., Li, J.-Y., Xu, R.-K., 2018. Preferential adhesion of surface groups of Bacillus subtilis on gibbsite at different ionic strengths and pHs revealed by ATR-FTIR spectroscopy. Colloids Surf. B: Biointerfaces 165, 83–91.

Horton, R., Horn, R., Bachmann, S., 2016. Essential Soil Physics: An Introduction to Soil Processes, Functions, Structure and Mechanics.

Huang, Y., Li, S., 2024. Overview of soil geography: definition, formation, functions, and prospects. Geogr. Res. Bull. 3, 60–79.

Huang, Z., Wang, Y., Guo, F., Ouyang, X., Zhu, Z., Zhang, Y., 2024. Mangrove soil carbon stocks varied significantly across community compositions and environmental gradients in the largest mangrove wetland reserve, China. Regional Environ. Chang. 24 (4), 140.

Inyang, E., 2011. Environmental Problems in the Bakossi Landscape: A Handbook for Environmental Educators. African Books Collective.

IUSS Working Group WRB, 2022. World reference base for soil resources. In: International Soil Classification System for naming Soils and Creating Legends for Soil Mpas.

Jackson, M.L., 1973. Soil chemical analysis-advanced course: A manual of methods useful for instruction and research in soil chemistry, physical chemistry of soils, soil fertility, and soil genesis, p. author.

Jones Jr., J.B., 1991. Kjeldahl method for nitrogen determination. Micro-Macro Publishing, Inc.

Joshi, R.K., Garkoti, S.C., 2023. Influence of vegetation types on soil physical and chemical properties, microbial biomass and stoichiometry in the central Himalaya. Catena 222, 106835.

Khan, F., Fenton, T., 1994. Saturated zones and soil morphology in a Mollisol catena of Central Iowa. Soil Sci. Soc. Am. J. 58, 1457–1464.

Klute, A., 1986. Methods of soil analysis, part 1. Agronomy 9.

Kome, G.K., Enang, R.K., Yerima, B.P.K., 2018. Knowledge and management of soil fertility by farmers in western Cameroon. Geoderma Reg. 13, 43–51.

Krasilnikov, P., Fontana, A., Labaz, B., Landi, A., Mermut, A.R., Smreczak, B., Pinheiro, C.R., Van Huyssteen, C.W., Monger, C., de Oliveira, F.P., 2022. Status and challenges of black soils.

Kunghe, G., Azinwi Tamfuh, P., Mamdem, L., Ndzana, G., Moundjeu, D., 2023. Morphology, physico-chemical characteristics, nutrient status and fertility capability classification of andosols under different land use systems in Foumbot (Cameroon Western Highlands). J. Atmos. Earth Sci. 7, 041. of 12, 2.

Łabaz, B., Kabała, C., Dudek, M., Waroszewski, J., 2019. Morphological diversity of chernozemic soils in South-Western Poland. Soil Sci. Annu. 70, 211–224.

Lesovaya, S., Goryachkin, S.V., Polekhovskii, Y.S., 2012. Soil formation and weathering on ultramafic rocks in the mountainous tundra of the Rai-Iz massif, Polar Urals. Eurasian Soil Sci. 45, 33–44.
Liles, G.C., Beaudette, D.E., O'Geen, A.T., Horwath, W.R., 2013. Developing predictive soil C models for soils using quantitative color measurements. Soil Sci. Soc. Am. J. 77, 2173–2181.
Liu, J., Liu, B., Liu, H., Zhang, F., 2024. Long-term cultivation drives soil carbon, nitrogen, and bacterial community changes in the black soil region of northeastern China. Land Degrad. Dev. 35, 428–441.
Lyu, H., Watanabe, T., Ota, Y., Hartono, A., Anda, M., Dahlgren, R.A., Funakawa, S., 2022. Climatic controls on soil clay mineral distributions in humid volcanic regions of Sumatra and Java, Indonesia. Geoderma 425, 116058. https://doi.org/10.1016/j.geoderma.2022.116058.
Madejová, J., 2003. FTIR techniques in clay mineral studies. Vib. Spectrosc. 31, 1–10.
Manju, C., 2002. Mineralogical, Morphological and Geochemical Studies on Kundara and Madayi Kaolins, Kerala.
Marta, S., Zimmer, A., Caccianiga, M., Gobbi, M., Ambrosini, R., Azzoni, R.S., Gili, F., Pittino, F., Thuiller, W., Provenzale, A., 2023. Heterogeneous changes of soil microclimate in high mountains and glacier forelands. Nat. Commun. 14, 5306.
Matus, F., Rumpel, C., Neculman, R., Panichini, M., Mora, M., 2014. Soil carbon storage and stabilisation in andic soils: a review. Catena 120, 102–110.
McCarthy, M.J., Dyer, T.D., 2019. Pozzolanas and pozzolanic materials. In: Lea's Chemistry of Cement and Concrete, 5, pp. 363–467.
McKeague, J., 1967. An evaluation of 0.1 M pyrophosphate and pyrophosphate-dithionite in comparison with oxalate as extractants of the accumulation products in podzols and some other soils. Can. J. Soil Sci. 47, 95–99.
McKeague, J., Day, Jh., 1966. Dithionite-and oxalate-extractable Fe and Al as aids in differentiating various classes of soils. Can. J. Soil Sci. 46, 13–22.
Mefire, A.N., Fouateu, R.Y., Njoya, A., Mache, J.R., Pilate, P., Hatert, F., Fagel, N., 2018. Mineralogy and geochemical features of Foumban clay deposits (West Cameroon): genesis and potential applications. Clay Miner. 53, 431–445.
Mehra, O., Jackson, M., 1960. Iron Oxide Removal from Soils and Clays by a Dithionite-Citrate System Buffered with Sodium Bicarbonate.
Merlin, N., Nogueira, B.A., de Lima, V.A., dos Santos, L.M., 2014. Application of fourier transform infrared spectroscopy, chemical and chemometrics analyses to the characterization of agro-industrial waste. Química Nova 37, 1584–1588.
Metson, A.J., 1957. Methods of chemical analysis for soil survey samples. Soil Sci. 83, 245.
Miller, M.P., Singer, M.J., Nielsen, D.R., 1988. Spatial variability of wheat yield and soil properties on complex hills. Soil Sci. Soc. Am. J. 52, 1133–1141.
Milne, Geoffry, 1935. Some suggested units of classification and mapping, particularly of East African soils. In: Soil Research. Supplements to the Proceedings of the International Society of Soil Science, pp. 183–198.
Molina, J.A., Martín-Sanz, J.P., Casermeiro, M.Á., Quintana, J.R., 2024. Soil depth and vegetation type influence ecosystem functions in urban greenspaces. Appl. Soil Ecol. 194, 105209.
Montanarella, L., Panagos, P., Scarpa, S., 2021. In: Dent, D., Boincean, B. (Eds.), The Relevance of Black Soils for Sustainable Development BT - Regenerative Agriculture. Springer International Publishing, Cham, pp. 69–79.
Nanzyo, M., 2002. Unique properties of volcanic ash soils. Glob. Environ. Res. English Ed. 6, 99–112.
Nayak, D., Sarkar, D., Das, K., Chatterjee, S., 1999. Studies on pedogenesis in a soil chronosequence in West Bengal. J. Indian Soc. Soil Sci. 47, 322–328.
Ndzana, G.M., Huang, L., Wang, J.B., Zhang, Z.Y., 2018. Characteristics of clay minerals in soil particles from an argillic horizon of Alfisol in Central China. Appl. Clay Sci. 151, 148–156. https://doi.org/10.1016/j.clay.2017.10.014.
Ndzana, G.M., Huang, L., Zhang, Z., Zhu, J., Liu, F., Bhattacharyya, R., 2019. The transformation of clay minerals in the particle size fractions of two soils from different latitude in China. CATENA 175, 317–328. https://doi.org/10.1016/j.catena.2018.12.026.
Ndzana, G.M., Zhang, Y., Yao, S., Hamer, U., Zhang, B., 2022. The adsorption capacity of root exudate organic carbon onto clay mineral surface changes depending on clay mineral types and organic carbon composition. Rhizosphere 23, 100545. https://doi.org/10.1016/j.rhisph.2022.100545.
Ngandeu-Mboyo, J., Yemefack, M., Yongue-Fouateu, R., Bilong, P., 2016. Erodibility of cultivated soils in the Foumbot Area (West Cameroon). Tropicultura 34.
Nizeyimana, E., 1997. A toposequence of soils derived from volcanic materials in Rwanda: morphological, chemical, and physical properties. Soil Sci. 162.
Nottingham, A.T., Whitaker, J., Turner, B.L., Salinas, N., Zimmermann, M., Malhi, Y., Meir, P., 2015. Climate warming and soil carbon in tropical rainforests: insights from an elevation gradient in the Peruvian Andes. Bioscience 65, 906–921.
Olivier, L., Ouafo, M.R., Ndjigui, P., Bitom, D., Mfoumbeng, M.P., 2023. Methodological approach for the evaluation and mapping of the agronomic suitability of soils in tropical zones: case study of the Bambouto volcanic massif (Western Cameroon) and the Bokito district (Central Cameroon). PLOS Sustain.Transform. 2, e0000067.
Parfitt, R., 2009. Allophane and imogolite: role in soil biogeochemical processes. Clay Miner. 44, 135–155.
Poulenard, J., Herbillon, A.J., 2000. Sur l'existence de trois catégories d'horizons de référence dans les andosols. Comptes Rend. l'Acad. Sci. Ser. IIA-Earth Planet. Sci. 331 (10), 651–657.
Rasmussen, C., Matsuyama, N., Dahlgren, R.A., Southard, R.J., Brauer, N., 2007. Soil genesis and mineral transformation across an environmental gradient on andesitic lahar. Soil Sci. Soc. Am. J. 71, 225–237.
Rezaei, H., Jafarzadeh, A.A., Alijanpour, A., Shahbazi, F., Kamran, K.V., 2015. Effect of slope position on soil properties and types along an elevation gradient of arasbaran forest, Iran. Int. J. Adv. Sci. Eng. Inform. Technol. 5, 449–456.
Rogora, M., Frate, L., Carranza, M., Freppaz, M., Stanisci, A., Bertani, I., Bottarin, R., Brambilla, A., Canullo, R., Carbognani, M., 2018. Assessment of climate change effects on mountain ecosystems through a cross-site analysis in the Alps and Apennines. Sci. Total Environ. 624, 1429–1442.
Rubinić, V., Lazarević, B., Husnjak, S., Durn, G., 2015. Climate and relief influence on particle size distribution and chemical properties of Pseudogley soils in Croatia. Catena 127, 340–348.
Salazar, R., Alegre, J., Pizarro, D., Duff, A.J., García, C., Gómez, C., 2024. Soil carbon stock potential in pastoral and silvopastoral systems in the Peruvian Amazon. Agrofor. Syst. 1–11.
Shoji, S., Dahlgren, R., Nanzyo, M., 1993. Morphology of volcanic ash soils. In: Developments in Soil Science. Elsevier, pp. 7–35.
Simmons, N., 1990. Characterization and Classification of some Soils of Hawaii with Andic and Oxic Properties. University of Hawai'i at Manoa.
Sims, J.T., 2000. Soil test phosphorus: Bray and Kurtz P-1. Methods of phosphorus analysis for soils, sediments, residuals, and waters, 13.
Sisay, M.G., Tsegaye, E.A., Tolossa, A.R., Nyssen, J., Frankl, A., Van Ranst, E., Dondeyne, S., 2024. Soil-forming factors of high-elevation mountains along the east African Rift Valley: the case of the Mount Guna volcano, Ethiopia. Soil Syst. 8, 38.
Stevens, P., Walker, T., 1970. The chronosequence concept and soil formation. Q. Rev. Biol. 45, 333–350.
Stoops, G., Sedov, S., Shoba, S., 2018. Regoliths and soils on volcanic ash. In: Interpretation of Micromorphological Features of Soils and Regoliths. Elsevier, pp. 721–751.
Tamrat, W.Z., Rose, J., Grauby, O., Doelsch, E., Levard, C., Chaurand, P., Basile-Doelsch, I., 2019. Soil organo-mineral associations formed by co-precipitation of Fe, Si and Al in presence of organic ligands. Geochim. Cosmochim. Acta 260, 15–28.
Tchekambou, A.N.T., Tchouankoue, J.P., Angue, M.A., Ngansop, C., Theodoro, S.H., 2014. Fertilizing Ferralitic Soils in Cameroon Using Basalt Powder from the Cameroon Volcanic Line: An Application with Maize Farming in South Cameroon. Presented at the II Congresso Brasileiro de Rochagem, p. 82.
Tchokona Seuwi, D., 2010. Volcanisme paléogène à récent du secteur du massif de Mbépit (plaine du Noun): pétrologie, minéralogie, géochimie isotopique, géochronologie et approche environnementale.
Tematio, P., Fritsch, E., Hodson, M.E., Lucas, Y., Bitom, D., Bilong, P., 2009. Mineral and geochemical characterization of a leptic aluandic soil and a thapto aluandic-ferralsol developed on trachytes in Mount Bambouto (Cameroon volcanic line). Geoderma 152, 314–323.
Tematio, P., Tsafack, E.I., Kengni, L., 2011. Effects of tillage, fallow and burning on selected properties and fertility status of Andosols in the Mounts Bambouto, West Cameroon. Agric. Sci. 2 (03), 334.
Temgoua, E., Djoukouo, J., Likeng, J.D., Tematio, P., 2014. Structural stability of andisols and andic Ferralsols from Mount Bambouto, west Cameroon highlands. Cameroon Journal of Experimental Biology 10 (1), 26–34.
Tong, Y., Sorokin, A., 2024. What are black soils and why are black soils important in multiregional aspects? Moscow Univ. Soil Sci. Bull. 79 (5), 603–607.
Torrent, J., Schwertmann, U., Fechter, H., Alferez, F., 1983. Quantitative relationships between soil color and hematite content. Soil Sci. 136, 354–358.
Tsai, C., Chen, Z., Kao, C., Ottner, F., Kao, S., Zehetner, F., 2010. Pedogenic development of volcanic ash soils along a climosequence in Northern Taiwan. Geoderma 156, 48–59.
Tsozué, D., Nghonda, J.P., Tematio, P., Basga, S.D., 2019. Changes in soil properties and soil organic carbon stocks along an elevation gradient at Mount Bambouto, Central Africa. Catena 175, 251–262.
Van Ranst, E., Doube, M., Mees, F., Dumon, M., Ye, L., Delvaux, B., 2019. Andosolization of ferrallitic soils in the Bambouto Mountains, West Cameroon. Geoderma 340, 81–93.
Vieira, C.B., Silva, G.H.M.C., Almeida, B.G.D., Pessoa, L.G.M., Freire, F.J., de Souza Junior, Freire, M.B.G.D. S., 2025. Saturated Hydraulic Conductivity of Nine Soils According to Water Quality. Soil Texture, and Clay Mineralogy. Agronomy 15 (4), 864.
Wagai, R., Kishimoto-Mo, A.W., Yonemura, S., Shirato, Y., Hiradate, S., Yagasaki, Y., 2013. Linking temperature sensitivity of soil organic matter decomposition to its molecular structure, accessibility, and microbial physiology. Glob. Chang. Biol. 19, 1114–1125.
Walkley, A., Black, I.A., 1934. An examination of the Degtjareff method for determining soil organic matter, and a proposed modification of the chromic acid titration method. Soil Sci. 37, 29–38.
Wandji, P., Bardintzeff, J., Ménard, J., Tchoua, F., 2000. The alkaline fassaite-bearing volcanic province of the Noun Plain (West-Cameroon). Neues Jahrbuch fur Mineralogie-Monatshefte 1–14.
Wandji, P., Tchokona Seuwui, D., Bardintzeff, J.-M., Bellon, H., Platevoet, B., 2008. Rhyolites of the Mbépit Massif in the Cameroon Volcanic Line: an early extrusive volcanic episode of Eocene age. Mineral. Petrol. 94, 271–286.
Wang, L., Lu, P., Feng, S., Hamel, C., Sun, D., Siddique, K.H., Gan, G.Y., 2024. Strategies to improve soil health by optimizing the plant–soil–microbe–anthropogenic activity nexus. Agric. Ecosyst. Environ. 359, 108750.
Watanabe, T., Ueda, S., Nakao, A., Ze, A.M., Dahlgren, R.A., Funakawa, S., 2023. Disentangling the pedogenic factors controlling active Al and Fe concentrations in soils of the Cameroon volcanic line. Geoderma 430, 116289.
Winkler, P., Kaiser, K., Kölbl, A., Kühn, T., Schad, P., Urbanski, L., Fiedler, S., Lehndorff, E., Kalbitz, K., Utami, S., 2016. Response of Vertisols, andosols, and Alisols to paddy management. Geoderma 261, 23–35.
Xiao, J., He, X., Hao, J., Zhou, Y., Zheng, L., Ran, W., Shen, Q., Yu, G., 2016. New strategies for submicron characterization the carbon binding of reactive minerals in

long-term contrasting fertilized soils: implications for soil carbon storage. Biogeosciences 13, 3607–3618.
Zehetner, F., Miller, W.P., West, L.T., 2003. Pedogenesis of volcanic ash soils in Andean Ecuador. Soil Sci. Soc. Am. J. 67, 1797–1809.
Zhang, Z.Y., Huang, L., Liu, F., Wang, M.K., Fu, Q.L., Zhu, J., 2017. The properties of clay minerals in soil particles from two Ultisols, China. Clay Clay Miner. 65, 273–285.
Zhang, Yong, An, C., Zhang, W., Zheng, L., Zhang, Yan-zhen, Lu, C., Liu, L., 2023. Drivers of mountain soil organic carbon stock dynamics: a review. J. Soils Sediments 23, 64–76.
Ziem à Bidias, L.A., Ilouga, D.C.I., Moundi, A., Nsangou, A., 2020. Inventory and assessment of the Mbepit Massif geomorphosites (Cameroon Volcanic Line): assets for the development of local geotourism. Geoheritage 12, 1–19.